Digest Journal of Nanomaterials and Biostructures Vol. 9, No. 1, January - March 2014, p. 333 - 336

ELECTROCHEMICAL BEHAVIOUR OF MICROCELLULAR CARBON IN ACIDIC & BASIC ELECTROLYTES

G. NAN[a], A. BACIU[a], Z. BORSOS[a], A. TILIAKOS[b], B. DOBRICA[b], I. STAMATIN[b*]
[a]*Petroleum-Gas University of Ploieşti, Physics Department, Bd. Bucureşti 39, Romania,*
[b]*University of Bucharest, Faculty of Physics, 3Nano-SAE Research Centre, Bucharest-Măgurele, Romania,*

Microcellular carbon is an advanced material exhibiting notable properties, such as high mechanical resistance, controlled porosity, biocompatibility and considerable thermal/electrical conductivity. The present work aims to assess the hydrogen storage capacity of microcellular carbon by studying the dependence of hydrogen adsorption mechanisms to the geometrical parameters of microcellular carbon structures of varying porosity and to the surface chemistry at the interface between the carbon structures and electrolytes of varying pH.

(Received January 20, 2014; Accepted March 3, 2014)

Keywords:Microcellular carbon, cyclic voltammetry, hydrogen storage capacity

1. Introduction

Hydrogen is an alternative to the fossil fuels being an energy carrier in sustainable economic models based exclusively on renewable and alternative energy sources, collectively branded as “Hydrogen Economy” [1-4].However, the main drawback in the practical use of hydrogen is the difficulty in storing it safely and economically [5–7]; thus, the design of a safe and cost-effective hydrogen storage device presents itself as a priority. Hydrogen physical adsorption on porous carbon materials provides a promising solution [8]. Electrochemical hydrogen storage in such materials depends on the physicochemical properties of the material, the nature and concentration of the electrolytic mediumand the potential cut-off of the associated electrochemical mechanisms[9].Unlike other forms, the microcellular structures (CMC)arereticulated carbons resulting from polymer pyrolysis, wherethe porous network is shaped by a highly infusible and stablecomponent, made of microparticles of inertmaterials inserted in the initial polymer matrix, forming an interconnected 3D graphitic-likemicrostructure arranged in a cellular fashion.This paper investigates the electrochemical hydrogen storage in micro/meso porous CMCsfrom pyrolysis of polyacrylonitrile powder (PAN) mixed with non-decomposable salts in two range of grain size. The electrochemical behaviourby Cyclic Voltammetry (CV) in common acid and base electrolytes shows a low double layer capacity and a hydrogen accumulation in the mesoporous structures.

2. Materials and methods

Synthesis of CMC was performed bypyrolysis of an initial polymer matrix mixed with inert materials of μm size, allowing for thecontrolled introduction ofmicro-cells into the 3D structure (Figure 1) [10].

* Corresponding author: istarom@3nanosae.org

Materials: Polyacrylonitrile(PAN) powder (SigmaAldrich). Sodium chloride(NaCl) powder of technical graded in two ranges:100-300 μm and less than 60 μm (CMC2).

Preparation of samples: PAN powder was mixed with 10% w/w of salt and thenshaped in discs (Dia30x3 mm) using a mold at 3000Kgf/cm^2. Samples are indexed as follows: CMC1- PAN and 10% salt graded in range 100-300 μm; CMC2-PAN and 10% salt graded in range <60μm.

Thermal treatment: Temperature was raised slowly to 400°C for 3 hours in ambient atmosphere (thermoxidation phase); the samples were kept at 400°C for 30 minutes forthermostabilization (closing pyridinic cycles). Temperature was raised to 700°C for an hour inan inert atmosphere (argon); the samples were kept at that temperature for 30 minutes and then cooled at room temperature. Salt was removed by multiplesonications in water until constant weight was reached [10].SEM micrography for CMCs reveals specific features dependent of the grain size filler (figure 1). CMC1 shows large voids with nondefined shape. CMC2 shows a spherulitic carbon material with a large distribution in grain size from few microns upt to 50-70 microns. Earlier reports shown the microstructures for CMC consists of fused graphitic and pyridinic cycles with large microstructural deffects and dangling bonds on their surface[10].

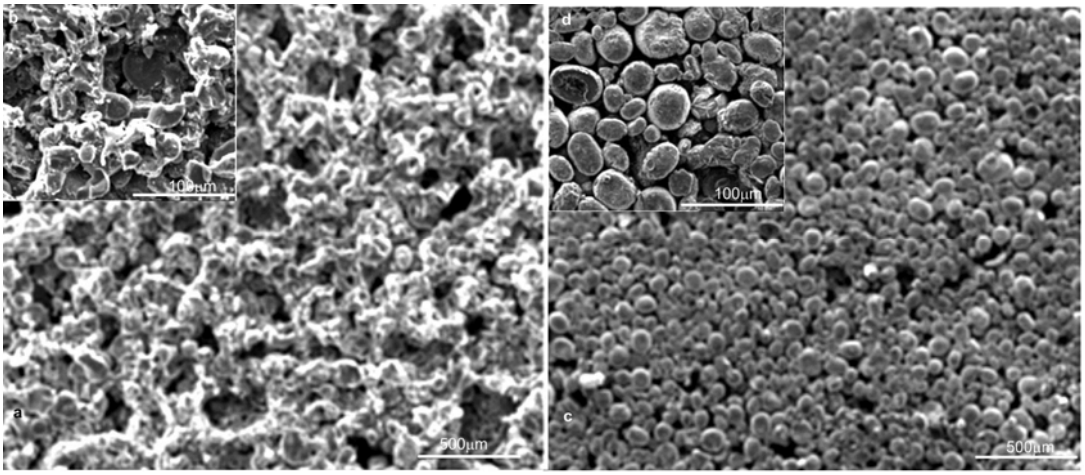

Fig. 1: SEM topography for CMC1 (a ,b) and CMC2 (c,d)[10]

Cyclic Voltammetry(CV):(VoltaLab 4.0 Analytical Radiometer, electrochemical method) at different scan rates, using6M NaOH and 0.5M H_2SO_4 electrolyte solutions. A simple three electrode configuration was employed for the electrochemical cell. The reference electrode, Ag/AgCl andCV scans were performed over a potential range from -1.5V to 1V using five different scan rates.

3. Results and discussion

3.1 Cyclic Voltammetry: basic electrolyte

CV profiles for CMC-*1*in a basic electrolyte of 6M NaOHare shown in Figure 2. Hydrogen is adsorbed in the cathodic direction and then oxidized in the anodic direction. Electrical double layer (EDL) and faradaic capacities for CMC-1,2 are small.In alkaline solutions the proton source is water which by electron transfer from active sites on the CMC surface lead to $2H_2O+2e^- \rightarrow H_2+2OH^-$ (-0.41 V vs SHE, reduction potential).Both voltammograms have two distinctive reduction peaks: 1) close to 0.25V vs Ag/AgCl assigned to hydrogen adsorption 2) close to -0.25V assigned to water splitting on the active sites and hydrogen accumulation in the mesoporous voids. This can be assigned to Heyrovsky mechanisms as CMC-$H_{ad}+H_2O+e^- \rightarrow H_2+OH^-$+CMC [11]. On the anodic component take place the oxidation reactions for hydrogen on different active sites.Due to heterogeneity in active sites developed on CMC surface during pyrolysis the current density

decreases with the scan rate from 10 mV/s to 5mV/s.Thus, the process is dominated by the kineticspath on the active sites at the electrode-electrolyte interface.

CV profiles for CMC-*2*in a basic electrolyte follow roughly the same patterns as for CMC-*1*(Figure 2). The transition from a larger cell sizeto a smaller one results in sharper redox peaks,a negligibleEDL and a small faradaic capacity.The most important peaks locatedin region 0.2-0.25 V respective -0.25 V/ vs Ag/AgCl can be assigned to hydrogen adsorption and hydrogen evolution based on Heyrovsky mechanisms.

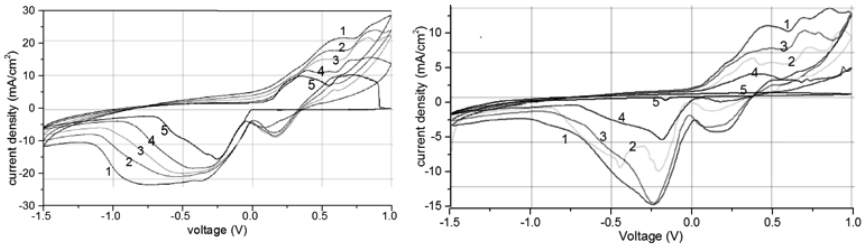

Fig. 2: CV profiles for CMC-1 (left) and CMC-2 (right) in 6M NaOH electrolyte. Scan rates: 1 - 100 mV/s, 2 - 50 mV/s, 3 - 25 mV/s, 4 - 10 mV/s and 5 - 5 mV/s.

Comparing profiles,at scan rate of 100 mV/s;thus as cellular structures become larger (and pore size increases), hydrogen storage capacity increases.

3.2 Cyclic Voltammetry: acidic electrolyte (0.5M H_2SO_4)

In acidic electrolyte the proton source is supplied by H_3O^+ and charge transfer steps take place on the most active sites with hydrogen adsorption (between 0.1-0. 25V vs Ag/AgCl) followed by electrolysis down -0.5V vs Ag/AgCl.CV profiles for CMC-*1*and CMC-2 in an acidic electrolyte (Figure 3) show a narrow electrical discharge layerand similar redox peaks associated with active centres on the CMC surface. Electrolysis is more pronounced at lower scan rates - at higher rates the intensity of the phenomenon decreases (CMC1) due to large pore size induced during pyrolysis.Current densities increase with the scan rate and the dominant mechanisms are quite different on the cathodic respective to anodic waves due to the active sites are quite different. CV profiles for CMC-*2*in an acidic electrolyte follow roughly the same patterns as for CMC-*1* (Figure 3).The electrical DL is almost non-existent in the oxidation regionand the phenomenon of electrolysis is dominant at all scan rates – instead, for CMC-*1* electrolysis is dominant at low scan rates, reducing in intensity when EDL capacity reaches its maximum value of 0.6 F/cm^2 at and above 50 mV/s scan rate.

Assessing the electric DL capacity at the reduction part of the profiles, we note that it reaches the value of 0.6 F/cm^{2}ata scan rate of 50 mV/s for CMC-*1*, but only reaches 0.3 F/cm^2 for CMC-*1*;thus again, hydrogen storage capacity increases according to the cellular size.

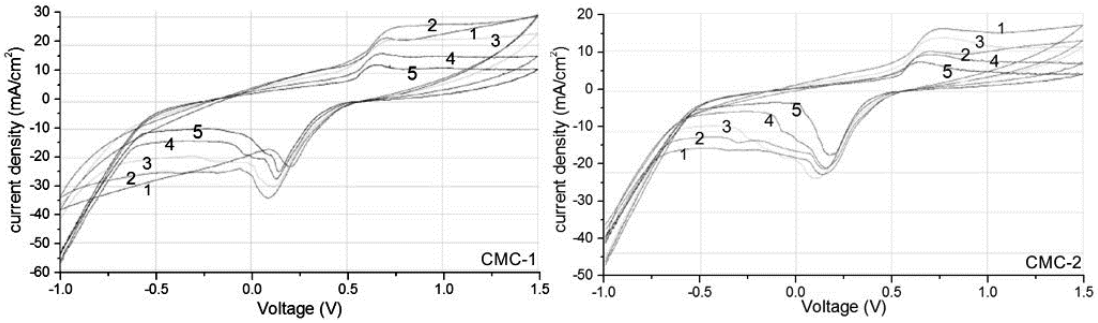

Fig. 3: CV profiles for CMC-1 (left) and CMC-2 (right) using a 0.5M H_2SO_4 electrolyte, Scan rates: 1 - 100 mV/s, 2 - 50 mV/s, 3 - 25 mV/s, 4 - 10 mV/s and 5 - 5 mV/s.

4. Conclusions

The present study assessed the feasibility of using microcellular carbon as hydrogen storage devices. CMCs obtained by pyrolysis of polyacrylonitrile powder mixed with non-decomposable saltscan be shaped in various microcellular structures (based on pore and cell size) and tested their electrochemical behaviour in basic and acidic electrolytes. Cyclic voltammogramsfor CMC in alkaline and acid electrolytesshow an electrochemical behaviourdependent of both cell/pore size. In alkaline electrolytes the hydrogen storage takes place in large pore sizei.e the electrolyte saturation.There is no electrolysis observed. In acid electrolyte dominant is hydrogen adsorption on the active sites and water electrolysis for CMC with small pore size (CMC2). The hydrogen storage capacity is not dominant in acidic electrolytes. The electrochemical behaviour of CMC is complex, due to the various active centres on its surface corresponding to various oxidation and reduction potentials respective due to a large volume of electrolyte which fill the pores. Low EDL and quite different electrochemical behaviour for both CMCs should be described in a new model based on 2D-3D fractal geometry.

Acknowledgement

The financial support of Romanian GrantsPN-II-ID-PCE-2011-3-0815 - contract no 64/2011, and by the SectorialOperational Programme Human Resources Development (SOP HRD),financed from the European Social Fund and by the Romanian Governmentunder the contract number SOP HRD/107/1.5/S/82514.

References

[1] L. Schlapbach and A. Züttel, Nature **414**(6861): 353 (2001).
[2] A. Züttel, A. Remhof, A. Borgschulte, O. Friedrichs, Philos. Trans. A Math. Phys. Eng. Sci.**368**(1923): 3329 (2010).
[3] B. Ewan, R. Allen, Inter. J. Hydrogen Energy**30**(8): 809 (2005).
[4] M. Ball, M. Wietschel (eds), The Hydrogen Economy: Opportunities and Challenges, Cambridge University Press, 2009.
[5] R. Ströbel, J. Garche, P.T. Moseley, L. Jörissen, G. Wolf, J. Power Sources 159, 781 (2006).
[6] Z. Li, Renew. Sust. Energy Rev.**9**(4): 395 (2005).
[7] G. Hermosilla-Lara, G. Momen, P. H. Marty, B. LeNeidre, K. Hassouni,, Int. J. Hydrogen Energy **32**(10-11): 1542 (2007).
[8] L. Schlapbach, A. Züttel, Nature**414**: 353 (2001).
[9] Y. Gogotsi (ed), Nanomaterials Handbook, CRC Press, Taylor & Francis Group, 2006.
[10] G. Nan, I. Stamatin, A. Andronie, Ş. Iordache, C. Cristescu, A. Cucu, A. Baciu, G. A. Rimbu, J. Optoelectron. Adv. Mater. **11**(11): 1788 (2009).
[11] K. Jurewicz, E. Frackowiak, F. Béguin, Appl. Phys. A**78**: 981 (2004).